La Celle, P. T., and Polakowska, R. R. (2001). Human homeobox HOXA7 regulates keratinocyte transglutaminase type 1 and inhibits differentiation. *J. Biol. Chem.* 276, 32844–32853. doi: 10.1074/jbc.M104598200

Lee, K. C., Li, C., Schneider, E. B., Wang, Y., Somervell, H., Krafft, M., et al. (2012). Is BRAF mutation associated with lymph node metastasis in patients with papillary thyroid cancer. *Surgery* 152, 977–983. doi: 10.1016/j.surg.2012.08.019

Loh, K. C., Greenspan, F. S., Gee, L., Miller, T. R., and Yeo, P. P. (1997). Pathological tumor-node-metastasis (pTNM) staging for papillary and follicular thyroid carcinomas: a retrospective analysis of 700 patients. *J. Clin. Endocrinol. Metab.* 82, 3553–3562. doi: 10.1210/jc.82.11.3553

Matsusaka, K., Kaneda, A., Nagae, G., Ushiku, T., Kikuchi, Y., Hino, R., et al. (2011). Classification of Epstein-Barr virus-positive gastric cancers by definition of DNA methylation epigenotypes. *Cancer Res.* 71, 7187–7197. doi: 10.1158/0008-5472.CAN-11-1349

McLeod, D. S., Sawka, A. M., and Cooper, D. S. (2013). Controversies in primary treatment of low-risk papillary thyroid cancer. *Lancet* 381, 1046–1057. doi: 10.1016/S0140-6736(12)62205-3

Mitsutake, N., Miyagishi, M., Mitsutake, S., Akeno, N., Mesa, C. Jr., Knauf, J. A., et al. (2006). BRAF mediates RET/PTC-induced mitogen-activated protein kinase activation in thyroid cells: functional support for requirement of the RET/PTC-RAS-BRAF pathway in papillary thyroid carcinogenesis. *Endocrinology* 147, 1014–1019. doi: 10.1210/en.2005-0280

Mohammadi-asl, J., Larijani, B., Khorgami, Z., Tavangar, S. M., Haghpanah, V., Kheirollahi, M., et al. (2011). Qualitative and quantitative promoter hypermethylation patterns of the P16, TSHR, RASSF1A and RARbeta2 genes in papillary thyroid carcinoma. *Med. Oncol.* 28, 1123–1128. doi: 10.1007/s12032-010-9587-z

Nagae, G., Isagawa, T., Shiraki, N., Fujita, T., Yamamoto, S., Tsutsumi, S., et al. (2011). Tissue-specific demethylation in CpG-poor promoters during cellular differentiation. *Hum. Mol. Genet.* 20, 2710–2721. doi: 10.1093/hmg/ddr170

Namba, H., Nakashima, M., Hayashi, T., Hayashida, N., Maeda, S., Rogounovitch, T. I., et al. (2003). Clinical implication of hot spot BRAF mutation, V599E, in papillary thyroid cancers. *J. Clin. Endocrinol. Metab.* 88, 4393–4397. doi: 10.1210/jc.2003-030305

Noguchi, S., Murakami, N., and Kawamoto, H. (1994). Classification of papillary cancer of the thyroid based on prognosis. *World J. Surg.* 18, 552–7. discussion: 8. doi: 10.1007/BF00353763

Noushmehr, H., Weisenberger, D. J., Diefes, K., Phillips, H. S., Pujara, K., Berman, B. P., et al. (2010). Identification of a CpG island methylator phenotype that defines a distinct subgroup of glioma. *Cancer Cell* 17, 510–522. doi: 10.1016/j.ccr.2010.03.017

Piccardo, A., Arecco, F., Puntoni, M., Foppiani, L., Cabria, M., Corvisieri, S., et al. (2013). Focus on high-risk DTC patients: high postoperative serum thyroglobulin level is a strong predictor of disease persistence and is associated to progression-free survival and overall survival. *Clin. Nucl. Med.* 38, 18–24. doi: 10.1097/RLU.0b013e318266d4d8

Schmidt, B., Liebenberg, V., Dietrich, D., Schlegel, T., Kneip, C., Seegebarth, A., et al. (2010). SHOX2 DNA methylation is a biomarker for the diagnosis of lung cancer based on bronchial aspirates. *BMC Cancer* 10:600. doi: 10.1186/1471-2407-10-600

Shaha, A. R., Shah, J. P., and Loree, T. R. (1996). Risk group stratification and prognostic factors in papillary carcinoma of thyroid. *Ann. Surg. Oncol.* 3, 534–538. doi: 10.1007/BF02306085

Shen, L., Toyota, M., Kondo, Y., Lin, E., Zhang, L., Guo, Y., et al. (2007). Integrated genetic and epigenetic analysis identifies three different subclasses of colon cancer. *Proc. Natl. Acad. Sci. U.S.A.* 104, 18654–18659. doi: 10.1073/pnas.0704652104

Suzuki, H., Gabrielson, E., Chen, W., Anbazhagan, R., van Engeland, M., Weijenberg, M. P., et al. (2002). A genomic screen for genes upregulated by demethylation and histone deacetylase inhibition in human colorectal cancer. *Nat. Genet.* 31, 141–149. doi: 10.1038/ng892

Tada, Y., Yokomizo, A., Shiota, M., Tsunoda, T., Plass, C., and Naito, S. (2011). Aberrant DNA methylation of T-cell leukemia, homeobox 3 modulates cisplatin sensitivity in bladder cancer. *Int. J. Oncol.* 39, 727–733. doi: 10.3892/ijo.2011.1049

Toyota, M., Ahuja, N., Ohe-Toyota, M., Herman, J. G., Baylin, S. B., and Issa, J. P. (1999). CpG island methylator phenotype in colorectal cancer. *Proc. Natl. Acad. Sci. U.S.A.* 96, 8681–8686. doi: 10.1073/pnas.96.15.8681

Ulisse, S., Baldini, E., Sorrenti, S., Barollo, S., Prinzi, N., Catania, A., et al. (2012). In papillary thyroid carcinoma BRAFV600E is associated with increased expression of the urokinase plasminogen activator and its cognate receptor, but not with disease-free interval. *Clin. Endocrinol. (Oxf.)* 77, 780–786. doi: 10.1111/j.1365-2265.2012.04465.x

Vogel, N., Schiebel, K., and Humeny, A. (2009). Technologies in the whole-genome age: MALDI-TOF-based genotyping. *Transfus. Med. Hemother.* 36, 253–262. doi: 10.1159/000225089

Weber, M., Hellmann, I., Stadler, M. B., Ramos, L., Paabo, S., Rebhan, M., et al. (2007). Distribution, silencing potential and evolutionary impact of promoter DNA methylation in the human genome. *Nat. Genet.* 39, 457–466. doi: 10.1038/ng1990

Weishaupt, J. H., Klocker, N., and Bahr, M. (2005). Axotomy-induced early down-regulation of POU-IV class transcription factors Brn-3a and Brn-3b in retinal ganglion cells. *J. Mol. Neurosci.* 26, 17–25. doi: 10.1385/JMN:26:1:017

Xing, M., Cohen, Y., Mambo, E., Tallini, G., Udelsman, R., Ladenson, P. W., et al. (2004). Early occurrence of RASSF1A hypermethylation and its mutual exclusion with BRAF mutation in thyroid tumorigenesis. *Cancer Res.* 64, 1664–1668. doi: 10.1158/0008-5472.CAN-03-3242

Xing, M., Haugen, B. R., and Schlumberger, M. (2013). Progress in molecular-based management of differentiated thyroid cancer. *Lancet* 381, 1058–1069. doi: 10.1016/S0140-6736(13)60109-9

Xing, M., Usadel, H., Cohen, Y., Tokumaru, Y., Guo, Z., Westra, W. B., et al. (2003). Methylation of the thyroid-stimulating hormone receptor gene in epithelial thyroid tumors: a marker of malignancy and a cause of gene silencing. *Cancer Res.* 63, 2316–2321.

Xing, M., Westra, W. H., Tufano, R. P., Cohen, Y., Rosenbaum, E., Rhoden, K. J., et al. (2005). BRAF mutation predicts a poorer clinical prognosis for papillary thyroid cancer. *J. Clin. Endocrinol. Metab.* 90, 6373–6379. doi: 10.1210/jc.2005-0987

Yagi, K., Akagi, K., Hayashi, H., Nagae, G., Tsuji, S., Isagawa, T., et al. (2010). Three DNA methylation epigenotypes in human colorectal cancer. *Clin. Cancer Res.* 16, 21–33. doi: 10.1158/1078-0432.CCR-09-2006

Yagi, K., Takahashi, H., Akagi, K., Matsusaka, K., Seto, Y., Aburatani, H., et al. (2012). Intermediate methylation epigenotype and its correlation to KRAS mutation in conventional colorectal adenoma. *Am. J. Pathol.* 180, 616–625. doi: 10.1016/j.ajpath.2011.10.010

Yamashita, H., Noguchi, S., Murakami, N., Watanabe, S., Uchino, S., Kawamoto, H., et al. (1998). Changing trends and prognoses for patients with papillary thyroid cancer. *Arch. Surg.* 133, 1058–1065. doi: 10.1001/archsurg.133.10.1058

Conflict of Interest Statement: The authors declare that the research was conducted in the absence of any commercial or financial relationships that could be construed as a potential conflict of interest.

Received: 21 September 2013; accepted: 18 November 2013; published online: 05 December 2013.

Citation: Kikuchi Y, Tsuji E, Yagi K, Matsusaka K, Tsuji S, Kurebayashi J, Ogawa T, Aburatani H and Kaneda A (2013) Aberrantly methylated genes in human papillary thyroid cancer and their association with BRAF/RAS mutation. Front. Genet. 4:271. doi: 10.3389/fgene.2013.00271

This article was submitted to Epigenomics and Epigenetics, a section of the journal Frontiers in Genetics.

progenitors express *bnl>GFP*. As progenitors continue along the DT, DT larval cells activate *bnl>GFP* expression one segment at a time from anterior to posterior, matching progenitor movement.

This dynamic *bnl* expression along the migration path is required for progenitor outgrowth. Knockdown of *bnl* expression by RNA interference (RNAi) in larval tracheal cells blocked migration and resulted in diminished or absent PAT (Fig. 3, B and C; fig. S7, A to C; and movie S2). Mosaic expression of *bnl RNAi* in small patches along the path (*23*) also arrested migration, so long as the patch encompassed the full DT circumference (Fig. 3D; fig. S7, D and E; and movies S3 and S4). Thus, Bnl is required all along the migration path, and the signal does not cross even short gaps.

Ectopic *bnl* expression in GFP-labeled clones of larval tracheal cells induced by *dfr-FLP* (*23*) redirected progenitor migration. Depending on the location of the clones, ectopic *bnl* caused incorrect exit from the niche, premature entry onto the DT, or wrong turns on the DT (Fig. 4, B to D). Dual clones induced bifurcation with groups of progenitors moving toward each ectopic *bnl* source (Fig. 4E). Clones in Tr3 and posterior metameres caused progenitors in these regions to leave the niche, even though they do not normally do so (Fig. 4, G and H, and fig. S8, D and E). When there was a large clone, progenitors migrated throughout the clone (Fig. 4F), implying that progenitors do not require a gradient and will spread to cover an entire region of cells expressing *bnl* at equivalent levels. When *bnl*-expressing clones failed to induce migration, the clones appeared to be too far from the progenitors or there was competition from another clone close by (fig. S8, A and B). Ectopic *bnl* expression within the progenitor cluster arrested migration (fig. S8C).

The results show that the embryonic tracheal inducer Bnl FGF guides tracheal progenitors out of the niche and into the posterior during tracheal metamorphosis. The source of Bnl is the larval tracheal branches destined for destruction, which serve both as the source of the chemoattractant and as the substratum for progenitor migration. Several days earlier in embryos, these larval tracheal branches were themselves induced by Bnl provided by neighboring tissues. But after embryonic development, most tracheal cells, including those in the decaying larval branches, downregulate *btl* FGFR expression (fig. S2A) and thus do not respond to (or sequester) the Bnl signal they later express. One of the most notable aspects of this larval Bnl is its exquisitely specific pattern in decaying larval branches, which presages progenitor outgrowth. It is unclear how Bnl expression is controlled, though it does not appear to require signals from migrating progenitors because the *bnl* reporter expression front progressed normally when progenitor outgrowth was stalled by a tracheal break (fig. S6C). Perhaps expression of Bnl involves gradients in the tracheal system or spatial patterning cues established during embryonic development in conjunction with temporal signals mediated by molting hormones.

Because the signal guiding progenitor migration is provided by tracheae destined for destruction, progenitors become positioned along the larval branches they replace (Fig. 4I). Perhaps during tissue repair and homeostasis, recruitment of adult stem or progenitor cells from the niche is similarly guided by signals from decaying tissue, thereby ensuring that new tissue is directed to the appropriate sites.

References and Notes

1. N. Barker, S. Bartfeld, H. Clevers, *Cell Stem Cell* **7**, 656–670 (2010).
2. G. B. Adams, D. T. Scadden, *Nat. Immunol.* **7**, 333–337 (2006).
3. A. Alvarez-Buylla, D. A. Lim, *Neuron* **41**, 683–686 (2004).
4. C. Blanpain, E. Fuchs, *Nat. Rev. Mol. Cell Biol.* **10**, 207–217 (2009).
5. E. Sancho, E. Batlle, H. Clevers, *Curr. Opin. Cell Biol.* **15**, 763–770 (2003).
6. G. L. Ming, H. Song, *Neuron* **70**, 687–702 (2011).
7. E. Nacu, E. M. Tanaka, *Annu. Rev. Cell Dev. Biol.* **27**, 409–440 (2011).
8. K. D. Poss, *Nat. Rev. Genet.* **11**, 710–722 (2010).
9. T. Matsuno, *Jap. J. Appl. Entomol. Zool.* **34**, 165–167 (1990).
10. G. Manning, M. A. Krasnow, in *The Development of* Drosophila melanogaster, M. Bate, A. Martinez-Arias, Eds. (Cold Spring Harbor Laboratory Press, Woodbury, NY, 1993), vol. 1, pp. 609–685.
11. M. Weaver, M. A. Krasnow, *Science* **321**, 1496–1499 (2008).
12. A. Guha, L. Lin, T. B. Kornberg, *Proc. Natl. Acad. Sci. U.S.A.* **105**, 10832–10836 (2008).
13. C. Pitsouli, N. Perrimon, *Development* **137**, 3615–3624 (2010).
14. M. Sato, Y. Kitada, T. Tabata, *Dev. Biol.* **318**, 247–257 (2008).
15. C. Ribeiro, M. Neumann, M. Affolter, *Curr. Biol.* **14**, 2197–2207 (2004).
16. L. Liu, W. A. Johnson, M. J. Welsh, *Proc. Natl. Acad. Sci. U.S.A.* **100**, 2128–2133 (2003).
17. K. Guillemin *et al.*, *Development* **122**, 1353–1362 (1996).
18. C. Klämbt, L. Glazer, B. Z. Shilo, *Genes Dev.* **6**, 1668–1678 (1992).
19. M. Reichman-Fried, B. Z. Shilo, *Mech. Dev.* **52**, 265–273 (1995).
20. D. Sutherland, C. Samakovlis, M. A. Krasnow, *Cell* **87**, 1091–1101 (1996).
21. J. Jarecki, E. Johnson, M. A. Krasnow, *Cell* **99**, 211–220 (1999).
22. M. Sato, T. B. Kornberg, *Dev. Cell* **3**, 195–207 (2002).
23. Materials and methods are available as supporting material on *Science* Online.
24. S. Hayashi *et al.*, *Genesis* **34**, 58–61 (2002).

Acknowledgments: We thank M. Weaver, M. Metzstein, and other lab members for advice and reagents. This work was supported by a Genentech Graduate Fellowship and a Ruth L. Kirschstein NIH training grant (F.C.) and the Howard Hughes Medical Institute.

Supplementary Materials

www.sciencemag.org/content/343/6167/186/suppl/DC1
Materials and Methods
Figs. S1 to S10
References (*25–39*)
Movies S1 to S4

4 June 2013; accepted 12 November 2013
10.1126/science.1241442

Mutational Analysis Reveals the Origin and Therapy-Driven Evolution of Recurrent Glioma

Brett E. Johnson,[1]* Tali Mazor,[1]* Chibo Hong,[1] Michael Barnes,[2] Koki Aihara,[3,4] Cory Y. McLean,[1]† Shaun D. Fouse,[1] Shogo Yamamoto,[3] Hiroki Ueda,[3] Kenji Tatsuno,[3] Saurabh Asthana,[5,6] Llewellyn E. Jalbert,[7] Sarah J. Nelson,[7,8] Andrew W. Bollen,[2] W. Clay Gustafson,[9] Elise Charron,[10] William A. Weiss,[1,9,10] Ivan V. Smirnov,[1] Jun S. Song,[11,12] Adam B. Olshen,[6,11] Soonmee Cha,[1] Yongjun Zhao,[13] Richard A. Moore,[13] Andrew J. Mungall,[13] Steven J. M. Jones,[13] Martin Hirst,[13] Marco A. Marra,[13] Nobuhito Saito,[4] Hiroyuki Aburatani,[3] Akitake Mukasa,[4] Mitchel S. Berger,[1] Susan M. Chang,[1] Barry S. Taylor,[5,6,11]‡ Joseph F. Costello[1]‡

Tumor recurrence is a leading cause of cancer mortality. Therapies for recurrent disease may fail, at least in part, because the genomic alterations driving the growth of recurrences are distinct from those in the initial tumor. To explore this hypothesis, we sequenced the exomes of 23 initial low-grade gliomas and recurrent tumors resected from the same patients. In 43% of cases, at least half of the mutations in the initial tumor were undetected at recurrence, including driver mutations in *TP53*, *ATRX*, *SMARCA4*, and *BRAF*; this suggests that recurrent tumors are often seeded by cells derived from the initial tumor at a very early stage of their evolution. Notably, tumors from 6 of 10 patients treated with the chemotherapeutic drug temozolomide (TMZ) followed an alternative evolutionary path to high-grade glioma. At recurrence, these tumors were hypermutated and harbored driver mutations in the RB (retinoblastoma) and Akt-mTOR (mammalian target of rapamycin) pathways that bore the signature of TMZ-induced mutagenesis.

The genetic landscape of tumors is continually evolving, which can be an impediment to the clinical management of cancer patients with recurrent disease (*1*, *2*). In contrast to the clonal evolution of hematological malignancies (*3*, *4*) and solid tumor metastases (*5–7*), the local regrowth of solid tumors after surgery occurs under a unique set of evolutionary pressures, which are further affected by adjuvant therapies. Through the acquisition of new mutations, residual tumor cells can progress to a more aggressive state. Grade II astrocytic gliomas are

particularly troublesome from this perspective. Although surgery is the standard of care, these invasive brain tumors typically recur (*8*). Many remain grade II at recurrence, while others progress to a higher histological grade with a poor prognosis (*9*). The incidence and timing of malignant progression are variable and unpredictable (*8*).

We undertook genome sequence analysis of initial and recurrent human gliomas to address two questions: (i) What is the extent to which mutations in initial tumors differ from their subsequent recurrent tumors? (ii) How does chemotherapy with temozolomide (TMZ), a drug commonly used in the treatment of glioma, affect the mutational profile of recurrent tumors? We sequenced the exomes of 23 grade II gliomas at initial diagnosis and their recurrences resected from the same patients up to 11 years later (table S1). We selected initial tumors of predominantly astrocytic histology that capture the full spectrum of glioma progression (histological grade II to IV at recurrence) and adjuvant treatment history. Tumor and matched normal DNA were sequenced to an average 125-fold coverage, enabling the sensitive detection of mutations down to a 10% variant frequency, small insertions and deletions, and DNA copy number alterations (CNAs) (Fig. 1A and tables S2 and S3) (*10*).

We identified an average of 33 somatic coding mutations in each initial tumor, of which an average of 54% were also detected at recurrence (shared mutations) (Fig. 1A). The shared mutations included those in *IDH1*, *TP53*, and *ATRX* in most but not all cases (fig. S1) (*11*–*13*). All other somatic mutations were identified only in the initial tumor or only in the recurrent tumor from a given patient (private mutations) and thus presumably arose later in tumor evolution. For example, mutations in *SMARCA4* were private to the initial or recurrent tumor in six of seven patients and therefore may confer a selective advantage in the context of preexisting early driver events (*14*, *15*). Overall, the initial and recurrent gliomas displayed a broad spectrum of genetic relatedness (fig. S2 and table S4). At one end of this spectrum were four patients whose tumors showed a pattern of linear clonal evolution; we infer that the recurrent tumors in these patients were seeded by cells bearing ≥75% of the mutations detected in the initial tumors (as in patient 27, Fig. 1B). At the other end of the spectrum, tumors from three patients showed branched clonal evolution; we infer that the recurrent tumors in these patients were seeded by cells derived from the initial tumor at an early stage of its evolution, as the recurrent tumors shared ≤25% of mutations detected in the initial tumors. Patient 17 was an extreme example of branched clonal evolution, as the initial and recurrent tumors shared only the *IDH1* R132H ($Arg^{132} \rightarrow$ His) mutation (Fig. 1C). This further implicates *IDH1* mutations as an initiating event in low-grade gliomagenesis (*12*). Indeed, *IDH1* mutation was the only shared mutation in every patient—an observation that supports the current interest in IDH1 as a therapeutic target (*16*). Paired tumors from the remaining 16 patients formed a continuum between linear and branched clonal evolution. Together, these data illustrate the extent to which genetically similar low-grade gliomas diverge after surgical resection, and suggest that recurrences may emerge from early stages in the evolution of the initial tumor.

Many solid tumors, including glioblastoma (GBM), display intratumoral heterogeneity (*17*, *18*). For example, geographically distinct parts of the tumor may have different mutations. Intratumoral heterogeneity could be a confounding factor in estimates of genetic divergence when only one relatively small fraction of a tumor is sampled. To explore the extent of intratumoral heterogeneity in our cases, we first analyzed the *BRAF* V600E ($Val^{600} \rightarrow$ Glu) mutation that was subclonal in the initial tumor of patient 18 and undetectable in the recurrent tumor by either exome sequencing or droplet digital polymerase chain reaction (PCR) (Fig. 1D and fig. S3) (*10*). *BRAF* V600E was present in three of six additional samples from geographically distinct regions of the initial tumor, whereas seven additional samples of the recurrence all lacked this mutation. These results suggest that the *BRAF*-mutant clone did not expand, despite the proliferative advantage typically conferred by this mutation. Such a finding contrasts sharply with the selection and outgrowth of subclonal drivers during the evolution of chronic lymphocytic leukemias (*3*).

Beyond the actionable *BRAF* mutation, we sequenced the exomes of additional, geographically distinct samples from three cases to further determine the extent to which apparently private mutations might be misclassified because of intratumoral heterogeneity. In patient 17, for whom all mutations except *IDH1* were private, intratumoral heterogeneity was observed in the initial and recurrent tumor. From the mutational profiles, however, we inferred that three samples of the initial tumor and four samples of the recurrence all derived from a common tumor cell of origin that possessed only an *IDH1* R132H mutation (Fig. 2A and table S5). Moreover, the recurrent tumor contained driver mutations in *TP53* and *ATRX* distinct from those observed in the initial tumor. We found no evidence of these new *TP53* or *ATRX* mutations in the initial tumor at allele frequencies of ~0.1% (figs. S3 and S4), implying convergent phenotypic evolution (*5*) via a strong ongoing selection for loss of these genes. The initial and recurrent tumors likely did not arise independently, as they also shared three somatic noncoding mutations (fig. S5). Thus, the initial and recurrent tumors were only distantly related and, despite the local and relatively rapid recurrence (fig. S6), exonic mutations other than *IDH1* R132H were only transiently present during the course of this patient's disease. Finally, we sequenced the exomes of additional distinct samples of the initial and recurrent tumors from patients 26 and 27, broadening our assessment of the impact of intratumoral heterogeneity on the reported genetic divergence. We found that only a small minority of private mutations were actually shared events (7%; table S3) (*10*). Intratumoral heterogeneity therefore could not explain the majority of the genetic divergence between the initial and recurrent tumors in our cohort, including the driver mutations in initial tumors that were undetected in their recurrence.

To investigate whether sequential recurrences from a single patient could each be traced to the same evolutionary stage of the initial tumor, we sequenced the exomes of the second and third recurrent tumors from patient 04 and constructed a disease phylogeny by clonal ordering (Fig. 2B, fig. S7, and table S5) (*5*, *19*). The initial tumor and three sequential local recurrences were clonally related, as indicated by the shared phylogenetic branch containing early driver mutations in *IDH1* and *TP53*. We infer that the tumor cells seeding the second recurrence branched off from the initial tumor at a slightly earlier evolutionary stage than the cells seeding the first recurrence. In contrast, the third recurrent tumor was a direct outgrowth of the second recurrence. These results show that branched and linear patterns of clonal evolution occurred at differing times in the same patient and are therefore not intrinsic properties of the tumor.

Beyond maximal, safe, surgical resection, there is currently no standard of care for patients with low-grade glioma; options include surveillance, adjuvant radiation alone, TMZ alone, or radiation and TMZ. TMZ is an alkylating agent that induces apoptosis in glioma cells and is sometimes used to defer or delay the use of radiation. However, there is currently no information on whether treatment of grade II astrocytomas with TMZ confers longer overall survival (*8*). Because TMZ is also mutagenic (*20*), we sought to determine how adjuvant chemotherapy with TMZ affects the mutational profile of recurrent tumors by comparing the initial low-grade gliomas to their recurrence after treatment. Although the initial tumors and most of the recurrent tumors in our cohort had 0.2 to 4.5 mutations per megabase (Mb) (*21*, *22*), 6 of the 10 patients treated with

[1]Department of Neurological Surgery, University of California, San Francisco, CA 94158, USA. [2]Department of Pathology, University of California, San Francisco, CA 94158, USA. [3]Genome Science Laboratory, Research Center for Advanced Science and Technology, University of Tokyo, Meguro-ku, Tokyo 153-8904, Japan. [4]Department of Neurosurgery, University of Tokyo, Bunkyo-ku, Tokyo 113-8655, Japan. [5]Department of Medicine, University of California, San Francisco, CA 94158, USA. [6]Helen Diller Family Comprehensive Cancer Center, University of California, San Francisco, CA 94158, USA. [7]Department of Bioengineering and Therapeutic Sciences, University of California, San Francisco, CA 94158, USA. [8]Department of Radiology and Biomedical Imaging, University of California, San Francisco, CA 94158, USA. [9]Department of Pediatrics, University of California, San Francisco, CA 94158, USA. [10]Department of Neurology, University of California, San Francisco, CA 94158, USA. [11]Department of Epidemiology and Biostatistics, University of California, San Francisco, CA 94158, USA. [12]Institute for Human Genetics, University of California, San Francisco, CA 94158, USA. [13]Michael Smith Genome Sciences Centre, British Columbia Cancer Agency, Vancouver, BC V5Z 4E6, Canada.

*These authors contributed equally to this work.
†Present address: 23andMe Inc., Mountain View, CA 94043, USA.
‡Corresponding author. E-mail: jcostello@cc.ucsf.edu (J.F.C.); barry.taylor@ucsf.edu (B.S.T.)

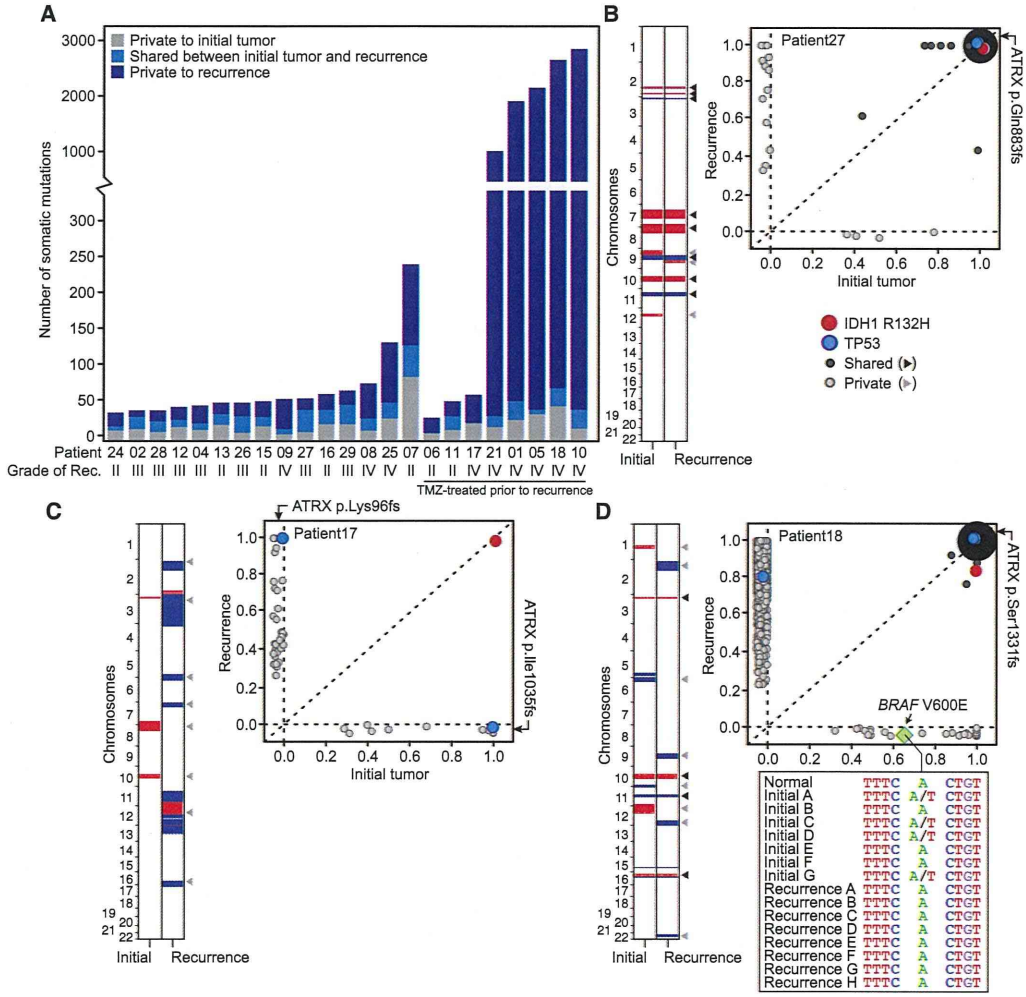

Fig. 1. Genetic landscapes of low-grade gliomas and their patient-matched recurrences. (**A**) Total number of mutations private to or shared between the initial and first recurrent glioma of 23 patients. (**B** to **D**) Shared and private somatic mutations in paired initial and recurrent tumors (*x* and *y* axes, respectively) as a function of the estimated fraction of tumor cells carrying the mutant allele. Mutations present in all the cells in both tumors are represented by a single point whose radius is scaled by the log count of such mutations. Shared and private CNAs are indicated (red and blue are gains and losses, respectively; white is copy-neutral). In (C), clonal *TP53* and *ATRX* mutations in the initial tumor were not identified in the recurrent tumor, but different clonal mutations in these two genes were acquired. (D) Inset shows the DNA sequence encompassing *BRAF* V600E in the normal tissue and in 15 geographically distinct samples of the initial and recurrent tumors.

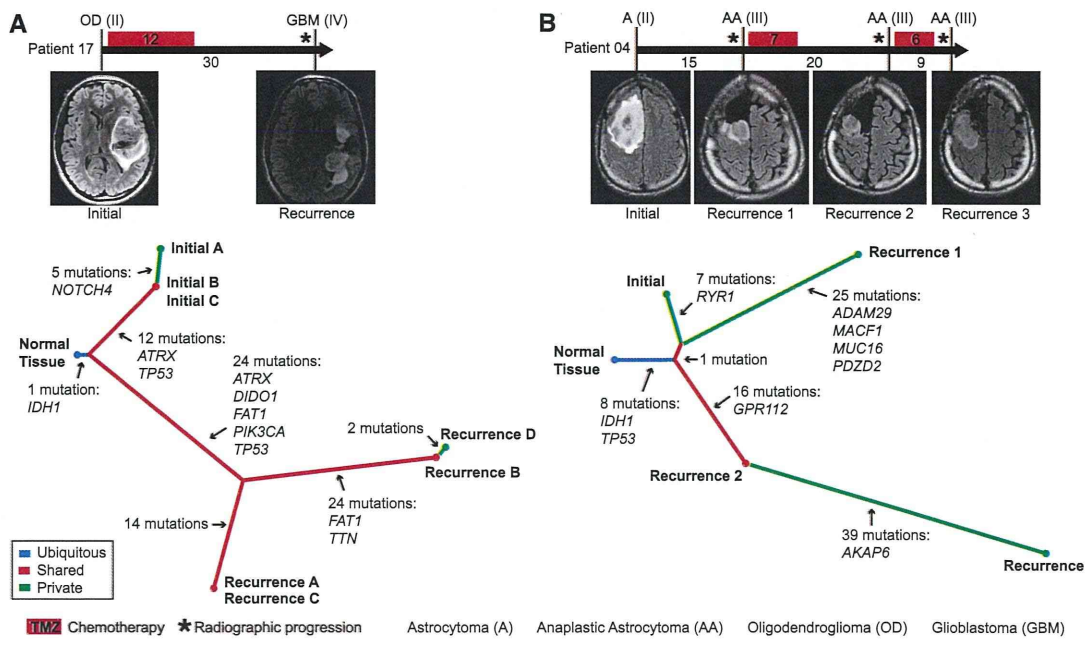

Fig. 2. Temporal and spatial patterns of clonal evolution in the tumors of two glioma patients. (**A** and **B**) A timeline of treatment histories for patient 17 (A) and patient 04 (B) (top, intervals labeled in months). Vertical bars correspond to the time of tumor resection and are labeled with the tumor diagnosis and grade. Representative MRIs are also shown. A phylogenetic tree (bottom) depicts the patterns of clonal evolution of these tumors inferred from the pattern and frequency of somatic mutations, highlighting genes frequently mutated in cancer.

TMZ had recurrent tumors that were hypermutated; that is, they harbored 31.9 to 90.9 mutations per Mb (table S6). Overall, 97% of these were C>T/G>A transitions predominantly occurring at CpC and CpT dinucleotides, which is a signature of TMZ-induced mutagenesis distinct from nonhypermutated tumors (fig. S8) (*20*, *22*, *23*). We classified C>T/G>A transitions in each hypermutated tumor as TMZ-associated if they were undetected in the matched initial tumor, which was resected before TMZ treatment (Fig. 3A). Although it is difficult to definitively attribute any single mutation to TMZ exposure, comparing the C>T/G>A mutation rates in each tumor pair suggested that >98.7% are due to TMZ-induced mutagenesis (*10*). To determine whether intratumoral heterogeneity in initial tumors resulted in the misclassification of some mutations as TMZ-associated, we sequenced the exomes of three additional geographically distinct samples of the untreated initial tumor from patient 18. For mutations classified as TMZ-associated, sequencing reads with the mutation were rare in the additional exomes and were found at rates no higher than expected by chance (1.7 ± 0.08%; P = 0.5, Wilcoxon rank-sum test) (*10*), further suggesting that they are induced by TMZ.

Resistance to TMZ develops in part through the acquisition of mutations that inactivate the DNA mismatch repair (MMR) pathway. MMR pathway dysfunction and continued TMZ exposure can in turn result in hypermutation (*22*–*25*). Indeed, we found that hypermutated tumors acquired somatic mutations in MMR genes that were not detected in their initial tumors, as well as aberrant DNA methylation of O^6-methylguanine-DNA methyltransferase (MGMT) (fig. S3, fig. S9, and table S1).

The introduction of thousands of de novo mutations may drive the evolution of TMZ-resistant glioma cells to higher states of malignant potential (*1*, *23*). Indeed, all six recurrent tumors that showed evidence of TMZ-induced hypermutation underwent malignant progression to GBM, a high-grade tumor with a worse prognosis (*8*, *9*). To investigate this hypothesis and to identify TMZ-associated mutations that may drive the outgrowth of GBM from low-grade glioma, we focused on the RB and Akt-mTOR signaling pathways, which are associated with high-grade gliomas (Fig. 3B) (*22*, *26*–*28*). In each hypermutated recurrence, TMZ-associated mutations affected genes coding for essential signaling molecules in these two pathways. For example, in the RB pathway we identified a TMZ-associated RB1 c.2520+1G>A splice-site mutation found previously in the germ line of patients with hereditary retinoblastoma (*29*, *30*). Transcriptome sequencing confirmed that this mutation triggered aberrant splicing, premature termination, and loss of the RB1 C-terminal domain necessary for growth suppression (Fig. 3C) (*31*). Recurrent tumors from patients 05 and 10 each had a TMZ-associated *CDKN2A* $Pro^{114} \rightarrow Leu$ mutation, which prevents $p16^{INK4A}$ protein encoded by this gene from inhibiting CDK4 or inducing cell cycle arrest (*32*). The same mutation has been reported in other tumor types (*33*) and in the germ line of patients with familial melanoma (*34*). Gene set enrichment analysis further confirmed the deregulation of RB1-mediated cell cycle control upon tumor recurrence (Fig. 3D), which suggests that TMZ-associated mutations compromise the function of the RB tumor suppressor pathway.

We also investigated TMZ-associated mutations that may activate the Akt-mTOR signaling pathway. We identified a TMZ-associated mutation (*PIK3CA* $Glu^{542} \rightarrow Lys$) in the recurrent tumor of patient 18 that drives Akt hyperactivation and induces mTOR-dependent oncogenic transformation (*35*). Similarly, the TMZ-treated second recurrence of patient 24 had TMZ-associated mutations in *PTEN* ($Ala^{121} \rightarrow Thr$ and $Gly^{165} \rightarrow Arg$) at residues critical to its phosphatase activity (*36*) that are recurrently mutated in GBM (*33*). Finally, we validated in vitro that a TMZ-associated *MTOR* S2215F ($Ser^{2215} \rightarrow Phe$) mutation in the recurrent tumor of patient 01 was constitutively

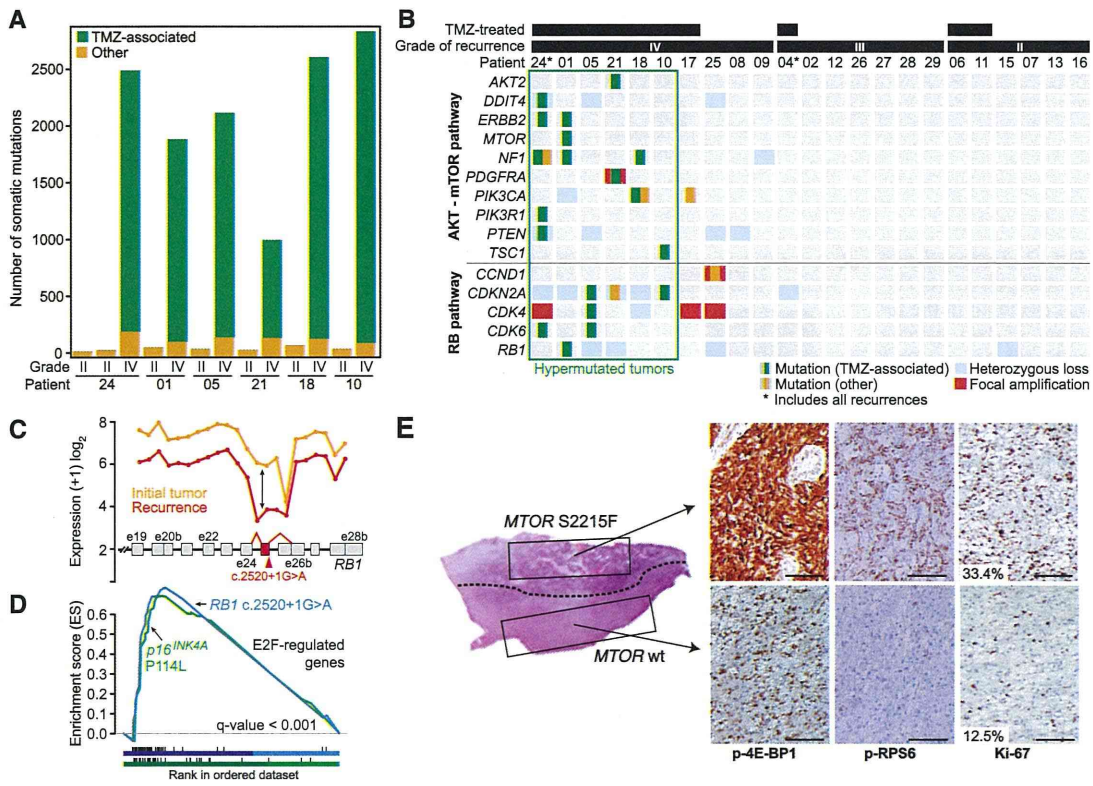

Fig. 3. Recurrent tumors from patients treated with TMZ harbor genetic alterations in the RB and Akt-mTOR signaling pathways. (**A**) Numbers of TMZ-associated mutations and other mutations identified in the six patients with hypermutated recurrent tumors. (**B**) Somatic mutations and CNAs acquired upon recurrence in key genes of pathways associated with GBM. (**C**) Expression level of *RB1* at each exon and exon-exon junction in the initial and recurrent tumor of patient 01 showing aberrant splicing of the *RB1* transcript in the recurrent tumor harboring the *RB1* c.2520+1G>A splice-site mutation. The *RB1* exon and exon junctions with significant differential usage (red) and the location of the splice-site mutation are shown. (**D**) Gene set enrichment analysis shows significant enrichment of genes down-regulated by *RB1* and up-regulated by *E2F* in the recurrent tumors of patients 01 (blue) and 10 (green), coincident with the acquisition of TMZ-associated mutations in the RB pathway. (**E**) Hematoxylin and eosin (H&E)–stained tumor sample from the first recurrent tumor of patient 01. A dotted line separates the two morphologically distinct regions. Immunohistochemistry (IHC) for phospho-RPS6, phospho-4E-BP1, and Ki-67 shows differential activation of mTORC1 targets and proliferation rates in the two adjacent regions. Scale bars, 100 μm.

activating (fig. S10), similar to the previously identified *MTOR* $Ser^{2215} \rightarrow$ Tyr (*37*). Moreover, adjacent regions of this recurrence showed heterogeneous mTOR complex 1 (mTORC1) activity (Fig. 3E and fig. S11). Microdissection revealed that although these adjacent regions shared a subset of the mutations found in the initial tumor, *MTOR* S2215F and other TMZ-associated mutations were present only in the region that stained strongly for mTORC1 activation, which also had higher staining of the proliferation marker Ki-67, implying that the TMZ-associated mutations conferred a proliferative advantage. A distal second recurrence harbored the same TMZ-associated mutations and stained strongly and homogeneously for mTORC1 targets (fig. S12). Although both regions of the first recurrence were GBM, the hypermutated subclone underwent in vivo selection, invaded distally, and seeded the second recurrence (figs. S13 and S14). Across our cohort, Akt-mTOR pathway mutations corresponded with elevated phospho-4E-BP1 and RPS6 in vivo, indicating hyperactivated mTORC1 in recurrent GBMs relative to their initial tumors (fig. S12).

There was no evidence that the mutations in the RB and Akt-mTOR signaling pathways preceded TMZ treatment, according to analysis of additional geographically distinct samples of initial tumors from four of the six patients with hypermutated recurrent tumors (table S7). Non-hypermutated recurrent tumors that progressed to GBM also acquired genetic changes in these signaling pathways, but through alternative mechanisms. In contrast, none of the grade II-III recurrences acquired mutations in these pathways. These data suggest a connection among TMZ treatment, driver mutations in oncogenic signaling pathways, and malignant progression.

Through direct comparison of the genomic landscape of gliomas at initial diagnosis and recurrence, we were able to infer the mutational character of the infiltrating tumor cells that give rise to recurrence and that adjuvant therapy with TMZ is intended to eliminate. Recurrences did not typically arise from cells bearing the full set of mutations found in the initial tumor, as would be expected from a local recurrence in the absence of selective pressure from adjuvant chemotherapy. This finding complicates the use of tumor genomics to design precision therapies targeting residual disease. We also demonstrated an alternative evolutionary path of low-grade glioma that is largely determined by adjuvant chemotherapy with TMZ. This extends earlier studies of primary GBMs (*23*, *25*), unpaired recurrent tumors (*22*), and a cell culture model (*20*). Future basic and clinical studies must weigh the initial antitumor effects of TMZ against the potential risk of inducing new driver mutations and malignant progression. Ultimately, a better understanding of the invading cells that give rise to recurrent tumors and the effect of adjuvant therapeutics on their evolution will facilitate the development of new strategies to delay or prevent recurrence and malignant progression.

References and Notes

1. M. Gerlinger, C. Swanton, *Br. J. Cancer* **103**, 1139–1143 (2010).
2. M. Greaves, C. C. Maley, *Nature* **481**, 306–313 (2012).
3. D. A. Landau *et al.*, *Cell* **152**, 714–726 (2013).
4. L. Ding *et al.*, *Nature* **481**, 506–510 (2012).
5. M. Gerlinger *et al.*, *N. Engl. J. Med.* **366**, 883–892 (2012).
6. S. Yachida *et al.*, *Nature* **467**, 1114–1117 (2010).
7. X. Wu *et al.*, *Nature* **482**, 529–533 (2012).
8. N. Sanai, S. Chang, M. S. Berger, *J. Neurosurg.* **115**, 948–965 (2011).
9. M. Westphal, K. Lamszus, *Nat. Rev. Neurosci.* **12**, 495–508 (2011).
10. See supplementary materials on *Science* Online.
11. Y. Jiao *et al.*, *Oncotarget* **3**, 709–722 (2012).
12. T. Watanabe, S. Nobusawa, P. Kleihues, H. Ohgaki, *Am. J. Pathol.* **174**, 1149–1153 (2009).
13. K. Watanabe *et al.*, *Clin. Cancer Res.* **3**, 523–530 (1997).
14. P. P. Medina *et al.*, *Hum. Mutat.* **29**, 617–622 (2008).
15. S. Glaros, G. M. Cirrincione, A. Palanca, D. Metzger, D. Reisman, *Cancer Res.* **68**, 3689–3696 (2008).
16. D. Rohle *et al.*, *Science* **340**, 626–630 (2013).
17. N. J. Szerlip *et al.*, *Proc. Natl. Acad. Sci. U.S.A.* **109**, 3041–3046 (2012).
18. A. Sottoriva *et al.*, *Proc. Natl. Acad. Sci. U.S.A.* **110**, 4009–4014 (2013).
19. L. M. F. Merlo, J. W. Pepper, B. J. Reid, C. C. Maley, *Nat. Rev. Cancer* **6**, 924–935 (2006).
20. W. J. Bodell, N. W. Gaikwad, D. Miller, M. S. Berger, *Cancer Epidemiol. Biomarkers Prev.* **12**, 545–551 (2003).
21. C. Greenman *et al.*, *Nature* **446**, 153–158 (2007).
22. Cancer Genome Atlas Research Network, *Nature* **455**, 1061–1068 (2008).
23. C. Hunter *et al.*, *Cancer Res.* **66**, 3987–3991 (2006).
24. D. P. Cahill *et al.*, *Clin. Cancer Res.* **13**, 2038–2045 (2007).
25. S. Yip *et al.*, *Clin. Cancer Res.* **15**, 4622–4629 (2009).
26. G. Reifenberger, J. Reifenberger, K. Ichimura, P. S. Meltzer, V. P. Collins, *Cancer Res.* **54**, 4299–4303 (1994).
27. H. Wang *et al.*, *Lab. Invest.* **84**, 941–951 (2004).
28. D. N. Louis, *Annu. Rev. Pathol.* **1**, 97–117 (2006).
29. T. Tsai *et al.*, *Arch. Ophthalmol.* **122**, 239–248 (2004).
30. C. Houdayer *et al.*, *Hum. Mutat.* **23**, 193–202 (2004).
31. X. Q. Qin, T. Chittenden, D. M. Livingston, W. G. Kaelin Jr., *Genes Dev.* **6**, 953–964 (1992).
32. J. Koh, G. H. Enders, B. D. Dynlacht, E. Harlow, *Nature* **375**, 506–510 (1995).
33. S. A. Forbes *et al.*, *Curr. Protoc. Hum. Genet.* Chapter 10, Unit 10.11 (2008).
34. M. C. Fargnoli *et al.*, *J. Invest. Dermatol.* **111**, 1202–1206 (1998).
35. S. Kang, A. G. Bader, P. K. Vogt, *Proc. Natl. Acad. Sci. U.S.A.* **102**, 802–807 (2005).
36. S. Y. Han *et al.*, *Cancer Res.* **60**, 3147–3151 (2000).
37. T. Sato, A. Nakashima, L. Guo, K. Coffman, F. Tamanoi, *Oncogene* **29**, 2746–2752 (2010).

Acknowledgments: We thank S. Gonzalez for assistance with the collection of clinical information; R. Kang for assistance with mutation validation; H. van Thuijl for assistance with MGMT methylation; and J. Wiencke and G. Hsuang for assistance with droplet digital PCR. Supported by Accelerate Brain Cancer Cure (J.F.C.), the Grove Foundation, the TDC Foundation, the Anne and Jason Farber Foundation, the Samuel Waxman Cancer Research Foundation, the Alex Lemonade Stand Foundation, the Entertainment Industry Foundation and Anne Feeley, and a generous gift from the Dabbiere family. Also supported by National Institute of General Medical Sciences grant T32GM008568 (T.M.); NIH grants 1T32CA15102201 and R25NS070680 (M.B.); NIH grant P50CA097257 (L.E.J., S.J.N., M.S.B., S.M.C., J.F.C., and B.S.T.); National Cancer Institute grants R01CA169316-01 (J.F.C.), P01CA81403 (W.C.G., E.C., and W.A.W.), P30CA82103 (A.B.O.), and R01CA163336 (J.S.S.); National Institute of Neurological Disorders and Stroke grant K08NS079485 (W.C.G., E.C., and W.A.W.); the UCSF Academic Senate and the Sontag Foundation (J.S.S., J.F.C., and B.S.T.); the BC Cancer Foundation, Genome BC, and Genome Canada (M.A.M.); the Goldhirsh Foundation (J.F.C.); and a research program of the Project for Development of Innovative Research on Cancer Therapeutics (P-Direct) (A.M., N.S., and H.A.), Grant-in-Aid for Scientific Research on Innovative Areas (no. 23134501) (A.M.), and Grant-in-Aid for Scientific Research (S) (no. 24221011) (H.A.) from the Ministry of Education, Culture, Sports, Science and Technology of Japan. C.Y.M. was a Damon Runyon Cancer Research Postdoctoral Fellow. M.A.M. is a Canada Research Chair in Genome Science. All exome and transcriptome sequencing data have been deposited in the European Genome-phenome Archive under accession number EGAS00001000579, and data from patients 24 to 29 have also been deposited to the Japanese Genotype-phenotype Archive under accession number JGAS00000000004.

Supplementary Materials

www.sciencemag.org/content/343/6167/189/suppl/DC1
Materials and Methods
Figs. S1 to S14
Tables S1 to S7
References (*38*–*61*)

2 May 2013; accepted 27 November 2013
Published online 12 December 2013;
10.1126/science.1239947

Single-Cell RNA-Seq Reveals Dynamic, Random Monoallelic Gene Expression in Mammalian Cells

Qiaolin Deng,[1]* Daniel Ramsköld,[1,2]* Björn Reinius,[1,2] Rickard Sandberg[1,2]†

Expression from both alleles is generally observed in analyses of diploid cell populations, but studies addressing allelic expression patterns genome-wide in single cells are lacking. Here, we present global analyses of allelic expression across individual cells of mouse preimplantation embryos of mixed background (CAST/Ei] × C57BL/6]). We discovered abundant (12 to 24%) monoallelic expression of autosomal genes and that expression of the two alleles occurs independently. The monoallelic expression appeared random and dynamic because there was considerable variation among closely related embryonic cells. Similar patterns of monoallelic expression were observed in mature cells. Our allelic expression analysis also demonstrates the de novo inactivation of the paternal X chromosome. We conclude that independent and stochastic allelic transcription generates abundant random monoallelic expression in the mammalian cell.

In diploid organisms, the zygote inherits one set of autosomal chromosomes from each parent. Although it is widely believed that transcription of autosomal genes occurs from both parental alleles, specific classes of genes have been shown to express only one, randomly

nature genetics

Recurrent mutations in multiple components of the cohesin complex in myeloid neoplasms

Ayana Kon[1], Lee-Yung Shih[2], Masashi Minamino[3], Masashi Sanada[1,4], Yuichi Shiraishi[5], Yasunobu Nagata[1], Kenichi Yoshida[1], Yusuke Okuno[1], Masashige Bando[3], Ryuichiro Nakato[3], Shumpei Ishikawa[6,7], Aiko Sato-Otsubo[1], Genta Nagae[8], Aiko Nishimoto[6], Claudia Haferlach[9], Daniel Nowak[10], Yusuke Sato[1], Tamara Alpermann[9], Masao Nagasaki[11], Teppei Shimamura[5], Hiroko Tanaka[12], Kenichi Chiba[5], Ryo Yamamoto[13], Tomoyuki Yamaguchi[13,14], Makoto Otsu[15], Naoshi Obara[16], Mamiko Sakata-Yanagimoto[16], Tsuyoshi Nakamaki[17], Ken Ishiyama[18], Florian Nolte[10], Wolf-Karsten Hofmann[10], Shuichi Miyawaki[18], Shigeru Chiba[16], Hiraku Mori[17], Hiromitsu Nakauchi[13,14], H Phillip Koeffler[19,20], Hiroyuki Aburatani[8], Torsten Haferlach[9], Katsuhiko Shirahige[3], Satoru Miyano[5,12] & Seishi Ogawa[1,4]

Cohesin is a multimeric protein complex that is involved in the cohesion of sister chromatids, post-replicative DNA repair and transcriptional regulation. Here we report recurrent mutations and deletions involving multiple components of the cohesin complex, including *STAG2*, *RAD21*, *SMC1A* and *SMC3*, in different myeloid neoplasms. These mutations and deletions were mostly mutually exclusive and occurred in 12.1% (19/157) of acute myeloid leukemia, 8.0% (18/224) of myelodysplastic syndromes, 10.2% (9/88) of chronic myelomonocytic leukemia, 6.3% (4/64) of chronic myelogenous leukemia and 1.3% (1/77) of classical myeloproliferative neoplasms. Cohesin-mutated leukemic cells showed reduced amounts of chromatin-bound cohesin components, suggesting a substantial loss of cohesin binding sites on chromatin. The growth of leukemic cell lines harboring a mutation in *RAD21* (Kasumi-1 cells) or having severely reduced expression of RAD21 and STAG2 (MOLM-13 cells) was suppressed by forced expression of wild-type RAD21 and wild-type RAD21 and STAG2, respectively. These findings suggest a role for compromised cohesin functions in myeloid leukemogenesis.

Recent genetic studies have led to the discovery of a number of new mutational targets in myeloid malignancies, unmasking unexpected roles for deregulated histone modification and DNA methylation in both acute and chronic myeloid neoplasms[1,2]. However, knowledge of the spectrum of gene mutations in myeloid neoplasms remains incomplete. We previously reported a whole-exome sequencing study of 29 paired tumor and normal samples of myeloid neoplasms with myelodysplastic features[3]. Although our major discovery was that frequent spliceosome mutations are uniquely associated with myelodysplasia phenotypes, we also identified hundreds of previously unreported gene mutations[3]. Most of those mutations affected single individuals only and are probably passenger changes. Therefore, their importance in leukemogenesis remains undetermined. However, through closer inspection of an updated list of mutations, including newly validated single-nucleotide variants, we identified additional recurrent mutations involving *STAG2*, a core component of the cohesin complex (Online Methods and **Supplementary Table 1**). In addition, we found that two other functionally related cohesin components, *STAG1* and *PDS5B*, were mutated in single specimens (**Supplementary Fig. 1**).

Cohesin is a multimeric protein complex that is conserved across species and is composed of four core subunits, SMC1, SMC3, RAD21

[1]Cancer Genomics Project, Graduate School of Medicine, The University of Tokyo, Bunkyo-ku, Tokyo, Japan. [2]Division of Hematology-Oncology, Department of Internal Medicine, Chang Gung Memorial Hospital, Chang Gung University, Taipei, Taiwan. [3]Research Center for Epigenetic Disease, Institute of Molecular and Cellular Biosciences, The University of Tokyo, Bunkyo-ku, Tokyo, Japan. [4]Department of Pathology and Tumor Biology, Graduate School of Medicine, Kyoto University, Yoshida-Konoe-cho, Kyoto-shi Sakyo-ku, Kyoto, Japan. [5]Laboratory of DNA Information Analysis, Institute of Medical Science, The University of Tokyo, Minato-ku, Tokyo, Japan. [6]Department of Pathology, The University of Tokyo, Bunkyo-ku, Tokyo, Japan. [7]Department of Genomic Pathology, Medical Research Institute, Tokyo Medical and Dental University, Bunkyo-ku, Tokyo, Japan. [8]Genome Science Division, Research Center for Advanced Science and Technology, The University of Tokyo, Meguro-ku, Tokyo, Japan. [9]Munich Leukemia Laboratory, Munich, Germany. [10]Department of Hematology and Oncology, University Hospital Mannheim, Mannheim, Germany. [11]Division of Biomedical Information Analysis, Department of Integrative Genomics, Tohoku Medical Megabank Organization, Tohoku University, Aoba-ku, Sendai, Japan. [12]Laboratory of Sequence Data Analysis, Human Genome Center, Institute of Medical Science, The University of Tokyo, Minato-ku, Tokyo, Japan. [13]Division of Stem Cell Therapy, Institute of Medical Science, The University of Tokyo, Minato-ku, Tokyo, Japan. [14]Stem Cell and Organ Regeneration Project, Exploratory Research for Advanced Technology (ERATO), Japan Science and Technology Agency (JST), Chiyoda-ku, Tokyo, Japan. [15]Stem Cell Bank, Center for Stem Cell Biology and Regenerative Medicine, Institute of Medical Science, The University of Tokyo, Minato-ku, Tokyo, Japan. [16]Department of Hematology, Faculty of Medicine, University of Tsukuba, Tsukuba, Ibaraki, Japan. [17]Division of Hematology, Department of Medicine, Showa University School of Medicine, Shinagawa-ku, Tokyo, Japan. [18]Division of Hematology, Tokyo Metropolitan Ohtsuka Hospital, Toshima-ku, Tokyo, Japan. [19]Hematology/Oncology, Cedars-Sinai Medical Center, Los Angeles, California, USA. [20]National University of Singapore, Cancer Science Institute of Singapore, Singapore. Correspondence should be addressed to S.O. (sogawa-tky@umin.ac.jp).

Received 15 February; accepted 24 July; published online 18 August 2013; doi:10.1038/ng.2731

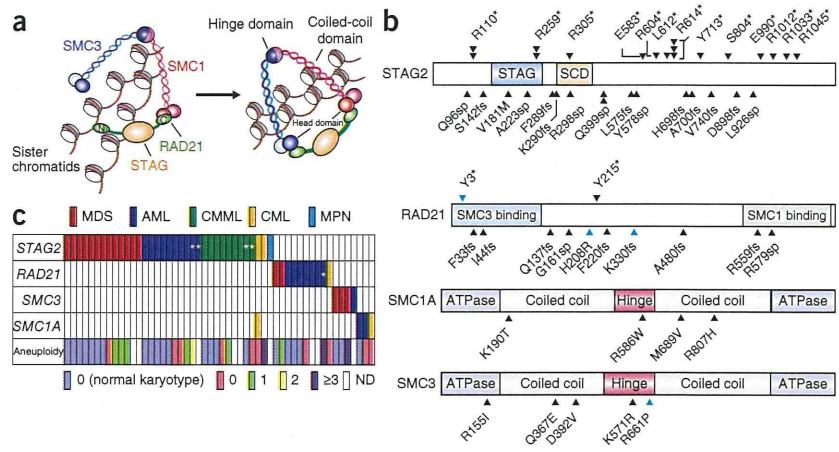

Figure 1 Genetic alterations of the cohesin complex in myeloid neoplasms. (**a**) Cohesin holds chromatin strands within a ring-like structure that is composed of four core components STAG, RAD21, SMC1 and SMC3. (**b**) Mutations in the core components of the cohesin complex found in myeloid malignancies (black arrowheads) and myeloid leukemia-derived cell lines (blue arrowheads). The amino acids in the alterations are referred to using their one-letter abbreviations (for example, R110* represents p.Arg110*). (**c**) Distribution of cohesin mutations and deletions showing a nearly mutually exclusive pattern among different myeloid neoplasms. Gene deletions are indicated by asterisks. The number of numerical chromosome abnormalities in each cohesin-mutated or -deleted case is shown at the bottom. ND, not determined.

and STAG proteins, together with a number of regulatory molecules such as PDS5, NIPBL and ESCO proteins (**Fig. 1a**)[4,5]. Forming a ring-like structure, cohesin is thought to be engaged in the cohesion of sister chromatids during cell division[5], post-replicative DNA repair[6,7] and the regulation of global gene expression through long-range *cis* interactions[8–12]. Germline mutations in cohesin components lead to the congenital multisystem malformation syndromes known as Cornelia de Lange syndrome and Roberts syndrome[13–15].

To investigate a possible role of cohesin mutations in myeloid leukemogenesis, we examined an additional 581 primary specimens of various myeloid neoplasms for mutations in nine cohesin or cohesin-related genes that have been implicated in mitosis[5] using high-throughput sequencing (**Supplementary Table 2**). We also investigated copy-number alterations in cohesin loci in 453 samples using SNP arrays (**Supplementary Table 3**). After excluding known and putative polymorphisms that are registered in the dbSNP or the 1000 Genomes project databases or that were predicted from multiple computational imputations, we identified a total of 60 nonsynonymous mutations involving nine genes in a total of 610 primary samples, which we validated by Sanger sequencing (**Fig. 1b** and **Supplementary Table 4**). After conservative evaluation of the probability of random mutational events across these genes, only four genes remained significantly mutated: *STAG2*, *RAD21*, *SMC1A* and *SMC3* ($P < 0.001$) (**Supplementary Table 5** and Online Methods). In addition, we detected five deletions in *STAG2* ($n = 4$) and *RAD21* ($n = 1$) (**Supplementary Fig. 2a,b** and **Supplementary Table 6**). We also found mutations in these four genes in four of the 34 myeloid leukemia cell lines studied (12%) (**Supplementary Table 7**).

We found mutations and deletions of these four genes in a mostly mutually exclusive manner in a variety of myeloid neoplasms, including acute myeloid leukemia (AML) (19/157), chronic myelomonocytic leukemia (CMML) (9/88), myelodysplastic syndromes (MDS) (18/224) and chronic myelogenous leukemia (CML) (4/64). Mutations were rate in classical myeloproliferative neoplasms (MPN) (1/77) (**Fig. 1c**, **Table 1** and **Supplementary Table 8**). In MDS, mutations were more frequent in refractory cytopenia with multilineage dysplasia and refractory anemia with excess blasts (11.4%) but were rare in refractory anemia, refractory anemia with ring sideroblasts, refractory cytopenia with multilineage dysplasia and ring sideroblasts and MDS with isolated del(5q) (4.2%) ($P = 0.044$). We also evaluated promoter methylation in 33 cases either with ($n = 12$) or without ($n = 21$) cohesin mutations or deletions for which sufficient nonamplified DNA was available using the HumanMethylation450 BeadChip; however, we found no aberrant methylations in cohesin loci, with the exception of hemimethylation of the *SMC1A* promoter that we found in two female cases (**Supplementary Fig. 3**).

We confirmed somatic origins for 17 mutations detected in 16 cases for which matched normal DNA was available (**Supplementary Table 4**). The somatic origins of an additional 23 mutations in *STAG2* or *SMC1A* found in 20 male cases were supported by the presence of reproducible wild-type signals or reads in Sanger and/or deep sequencing of the tumor samples, which were considered to originate from the X chromosome of the residual normal cells (**Supplementary Fig. 4**). In addition, for 20 mutations, the observed allele frequencies determined by pyrosequencing, deep sequencing or digital PCR showed significant deviations from the expected value for polymorphisms in the absence of apparent chromosomal alterations in a SNP array analysis ($P < 0.01$) (**Supplementary Figs. 5** and **6** and **Supplementary Tables 9–12**), suggesting their somatic origins. In addition, 32 of the 33 *STAG2* mutations and all of the nine *RAD21* mutations were either nonsense ($n = 18$), frameshift ($n = 14$) or splice-site ($n = 9$) changes, which were predicted to cause premature truncation of the protein or abnormal exon skipping (**Fig. 1b** and **Supplementary Figs. 7** and **8**). Thus, we considered the majority of the mutations to represent functionally relevant changes, probably of somatic origins (**Supplementary Table 13**).

Most of the cohesin mutations and deletions were heterozygous, except for the *STAG2* and *SMC1A* mutations on the single X chromosome in male cases ($n = 23$). In female samples, the *STAG2* promoter

Table 1 Frequencies of mutations and deletions of cohesin components in 610 myeloid neoplasms

Disease type	*n*	*STAG2*	*RAD21*	*SMC1A*	*SMC3*	Total	Percentage
MDS	224	13	2	0	3	18	8.0
CMML	88	9[a]	0	0	0	9	10.2
AML	157	10	7	2	1	19	12.1
de novo AML	120	8[a]	6	2	1	16	13.3
AML/MRC	37	2[a]	1[a]	0	0	3	8.1
CML	64	2[b]	1	2[b]	0	4	6.3
MPN	77	1	0	0	0	1	1.3
Total	610	35[b]	10	4[b]	4	52	8.5

Diseases are classified according to the World Health Organization 2008 classification. AML/MRC, AML with myelodysplasia-related changes.
[a]Two of the nine cases with *STAG2* alterations in CMML, one of the eight cases with *STAG2* alterations in *de novo* AML, one of the two cases with *STAG2* alterations in AML/MRC cases and one case with *RAD21* alteration in AML/MRC case involved genetic deletions. [b]One CML case having mutations in both *STAG2* and *SMC1A* was counted as a single case. A more detailed list is available in **Supplementary Table 8**.

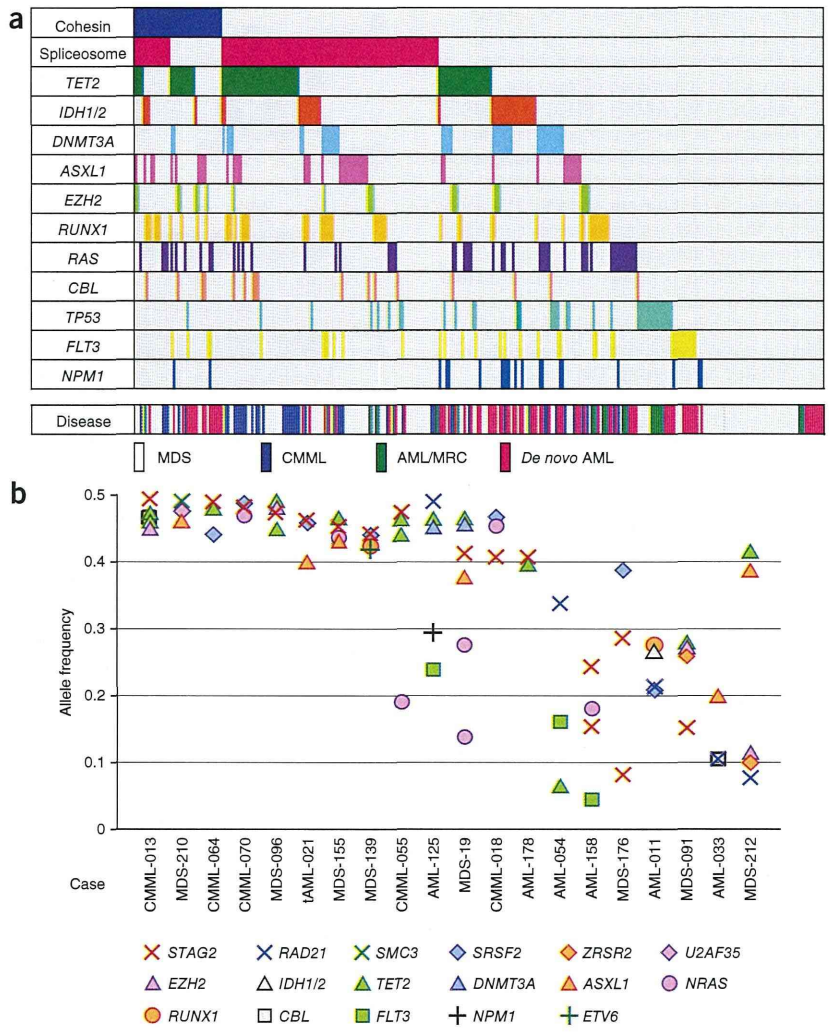

Figure 2 Relationship between cohesin mutations and other common mutations in myeloid malignancies. (**a**) Mutations in the cohesin complex and other common targets in 310 cases with different myeloid neoplasms. The corresponding disease types are shown in the bottom lane. *IDH1/2*, either *IDH1* or *IDH2*. AML/MRC, AML with myelodysplasia-related changes. (**b**) Allele frequencies of mutations in cohesin components and other coexisting mutations in 20 myeloid neoplasms determined by deep sequencing.

was hemimethylated through X inactivation regardless of mutation status (**Supplementary Fig. 3**), and a heterozygous mutation of the unmethylated *STAG2* allele would lead to biallelic *STAG2* inactivation, as has been previously documented in a female case with Ewing's sarcoma[16] and was also confirmed in a single case (CMML-036) in our cohort (**Supplementary Fig. 9**).

Cohesin mutations frequently coexisted with other mutations that are common in myeloid neoplasms and significantly associated with mutations in *TET2* ($P = 0.027$), *ASXL1* ($P = 0.045$) and *EZH2* ($P = 0.011$) (**Fig. 2a**). We performed deep sequencing of the mutant alleles in 20 available samples with cohesin mutations, which allowed for accurate determination of their allele frequencies. The majority of the cohesin mutations (15/20) existed in the major tumor populations, indicating their early origin during leukemogenesis. In the remaining five samples, we found cohesin mutations only in a tumor subpopulation, indicating that the mutations were relatively late events (**Fig. 2b**). Two male cases (MDS-176 and AML-158) harbored two independent subclones with different *STAG2* mutations, indicating that *STAG2* mutation could confer a strong advantage to pre-existing leukemic cells during clonal evolution (**Supplementary Fig. 10**). The number of mutations determined by whole-exome sequencing[3] was significantly higher in four cases with cohesin mutation or deletion compared to cases with no mutation or deletion of cohesin ($P = 0.049$) (**Supplementary Fig. 11**).

Next we investigated the possible impact of mutations on cohesin function. We examined the expression of STAG1, STAG2, RAD21, SMC3, SMC1A and NIPBL in 17 myeloid leukemia cell lines with ($n = 4$) or without ($n = 13$) known cohesin mutations, as well as in the chromatin-bound fractions of 13 cell lines (**Fig. 3a–d** and **Supplementary Table 14**)[14,17–19]. Although we observed an evaluable reduction in RAD21 expression in Kasumi-1 cells that harbored a frameshift alteration in RAD21 (p.Lys330ProfsX6) (**Fig. 3a**), alterations in P31FUJ (RAD21 p.His208Arg), CMY (RAD21 p.Tyr3X) and MOLM-7 (SMC3 p.Arg661Pro) cells were not accompanied by measurable decreases in the corresponding mutated proteins compared to wild-type cell lines. In contrast, we observed severely reduced expression of one or more cohesin components in KG-1 (STAG2)[16] and MOLM-13 (STAG1, STAG2, RAD21 and NIPBL) cells without any accompanying mutations in the relevant genes (**Fig. 3a**). We found no significant differences in protein expression of the cohesin components in cohesin-mutated and non-mutated cell lines in whole-cell extracts (**Fig. 3b**). However, expression of one or more cohesin components, including SMC1, SMC3, RAD21 and STAG2, was significantly reduced in the chromatin-bound fractions of cell lines with mutated or reduced expression of cohesin components, including Kasumi-1, KG-1, P31FUJ, MOLM-7 and MOLM-13 cells, compared with the cell lines with no known cohesin mutations or abnormal cohesin expression ($P < 0.05$), suggesting a substantial loss of cohesin-bound sites on chromatin (**Fig. 3c,d** and **Supplementary Table 14**)[14].

We next examined the effect of forced expression of wild-type cohesin components on the proliferation of a cohesin-mutated cell line (Kasumi-1) or a cell line with reduced expression of cohesin components (MOLM-13). Forced expression of wild-type *RAD21* and/or *STAG2*, but not of a truncated *RAD21* allele, induced significant growth suppression of the Kasumi-1 (with mutated *RAD21*) and MOLM-13 (with severe reduction of RAD21 and STAG2 expression) cell lines but not the K562 and TF1 (with wild-type *RAD21*) cell lines, supporting a leukemogenic role for compromised cohesin functions (**Fig. 4a–c** and **Supplementary Fig. 12a–g**). To explore the effect of forced expression of RAD21 on global gene expression, we performed expression microarray analysis of *RAD21*- and mock-transduced Kasumi-1 cells. In agreement with previous experiments with other cohesin and cohesin-related components, the magnitudes of the